Simple Loran Cycle Error Detection Algorithms for Maritime Harbor Entrance Approach Operations

Benjamin B. Peterson, Sherman C. Lo, Per K. Enge, *Stanford University*

ABSTRACT

Enhanced Loran (*eLoran*) is designed to support maritime harbor entrance approach (HEA) operations. As a result, the Radio Technical Commission for Maritime Services (RTCM) special committee 127 (SC127) is developing minimum performance specifications (MPS) for HEA *eLoran* receiver. The MPS specify required algorithms and processes to ensure safe operations of the receiver. One important algorithm is the high integrity determination of the tracked Loran cycle. This paper details and examines some of the algorithms being developed and analyzed by SC127.

SC 127 is developing simplified *eLoran* cycle error detection algorithms for the *eLoran* HEA MPS. Correct Loran cycle selection is needed to ensure safety as a cycle selection error results in range errors of 3 km or more. As HEA operations require accuracy levels of 10 meters, such errors pose a significant hazard. While other high integrity Loran cycle error detection algorithms have been proposed, these are require complex calculations and significant processing. The use of differential Loran in HEA supported areas can be leveraged to create a significantly simpler algorithm allowing for easier and lower cost implementation.

This paper develops and examines two simplified algorithms for cycle error detection for HEA. These algorithms use receiver autonomous integrity monitoring (RAIM) basic techniques of residual error and solution separation. The paper describes the algorithms, their implementation and demonstrates its capabilities in the conterminous United States (CONUS).

The goal of the work is to provide and demonstrate feasible algorithms for manufacturers to use for their MPS compliant HEA receiver.

INTRODUCTION

Cycle error and its detection is an essential step needed in processing the Loran signal and determining an accurate time of arrival (TOA) or time difference of arrival (TDOA). Loran receivers all perform some form of cycle identification. However, when we use Loran for safety of life applications such as non precision approach (NPA) or harbour entrance and approach (HEA), the fidelity of the cycle determination needs to be demonstrated.

Early in the Federal Aviation Administration (FAA) Loran Evaluation program it was recognized that proving cycle integrity to the required level was going to be the most difficult task in the program. We developed a residual test using a weighted sum of squared errors (WSSE) approach. [1]. Since this was first developed nearly six years ago, we have noted issues with the approach. The first was complexity. It required the calculation cumulative distribution functions (cdf) of χ^2 squared distributions with and without a non centrality parameter. Even then we could not accurately model distribution of sum of bias and noise. Bias errors are not known as so overbounds and conservative combinations had to be determined. This further increased complexity and resulted in significant conservatism. The complexity of the WSSE algorithm is a consequence of the integrity requirements for aviation and because of the significant residual range error and biases of *eLoran* implemented for aviation. Both these requirements are different under HEA. In HEA, differential corrections are provided resulting in significantly lower levels of error. The second major issue was performance. Because of large variation in signal to noise ratio (SNR) among stations, weak signals weighted out of the WSSE test statistic, and cycle errors on these most vulnerable signals became undetectable. These issues made it desirable to develop a simpler, better performing approach to proving cycle integrity and two such approaches are presented here.

Two detection algorithms based on redundancy on measurements and hypothesis testing were developed. Simplification is possible as nominal differentially corrected ranges have errors of a few meters compared to incorrect cycle selection which have errors of kilometers. Both methods are based on techniques used traditionally by receiver autonomous integrity monitoring (RAIM) algorithms. The first method performs a test on the sum squared error (SSE) or residuals. The second method is

based on multiple hypothesis solution separation (MHSS) techniques. This technique calculates solutions based on multiple subsets of ranging signals and examines their solution differences.

SUM SQUARED ERROR (SSE) OR RESIDUALS APPROACH

Deriving the sum squared error approach starts with calculating G, the geometry or direction cosine matrix. The calculation of the i^{th} row of the standard n x 3 matrix of direction cosines is given by Equation 1 with Az_i being the azimuth to the i^{th} station.

$$G(i,1:3) = [\cos(Az_i) \;\; \sin(Az_i) \;\; 1] \qquad (1)$$

If R_e is pseudorange error vector, the Least Squares position error vector (P_e) is given by Equation 2.

$$P_e = (G^T G)^{-1} G^T R_e \qquad (2)$$

The residual vector (R) is given by Equation 3.

$$R = R_e - G P_e = (I - G (G^T G)^{-1} G^T) R_e = A R_e \qquad (3)$$

This observability matrix, given by Equation 4, provides the desired mapping from range error to residuals.

$$A = I - G (G^T G)^{-1} G^T \qquad (4)$$

This matrix, A, is a function of only geometry. It will tell us:

- Which geometries will or will not allow us to detect a single cycle or larger (i.e. skywave) error.
- Which individual errors are detectable & which are not.
- Which geometries will or will not allow us to detect double cycle errors.
- Which combinations of two errors are detectable and which are not.

For fault free measurements, we will assume the sum of bias and noise on each pseudorange has bound to some required integrity bound. This simplifying assumption eliminates the calculation of chi square distributions. In the HEA case, differential Loran and a 25 m alarm limit, this bound has to be or order of 30-50 nanoseconds (ns) or less or fault free case will not meet requirement. Off-shore and non differential *eLoran*, this bound will be 300-500 ns.

SOLUTION SEPARATION APPROACH

Another approach commonly employed in RAIM is multiple hypothesis solution separation or, simply, solution separation (SS) [2][3]. Under solution separation, a comparison is conducted in the position domain amongst the solutions generated the various subset combination of measurements. The maximum difference between solutions is the metric for determining whether a fault (or multiple faults) has occurred. Solution separation can also be used for fault exclusion.

UNDERLYING EQUATIONS

Solution separation can be applied to Loran cycle integrity [4]. The basic formulation is to calculate the difference between the solution using subset i and j, z_{ij}. This is done for all combinations of different subsets. The technique can be assessed in a similar method. Equation 5 shows how to calculate z_{ij} where G is the geometry matrix, G_i, is the geometry matrix of i^{th} subset and ε is the error vector. It is easier to keep G_i the same size as G but zero out the rows corresponding to stations that are not part of the subset. To examine the capabilities of solution separation, we need to compare the nominal error or fault free case with faulted (cycle slip) cases. Under fault free conditions, the error can be both random and biases (*r, b*, respectively). The effects of these two forms of error are separated out to determine the solution separation under this condition. This is seen in Equation 6. We conduct two analysis steps to determine the effects of the bias and random errors, respectively. For the effect of bias, determine the error of each subset solution for each permutation of the biases. From the results, the maximum solution separation for the bias case is found. Biases are assumed to be at their maximum level and so only the relative direction or sign of the bias is of concern. There are 2^{n-1} different combinations of relative signs. The second step is to look at the effect of random noise. This is accomplished by examining the variance of each subset solution when differenced with the other subset solutions. This is seen in Equation 7. Hence we derive the bias and variance of each possible solution separation.

$$\begin{aligned} z_{ij} &= \left(G_i^T G_i\right)^{-1} G_i^T \varepsilon - \left(G_j^T G_j\right)^{-1} G_j^T \varepsilon \\ z_{ij} &= \left[\left(G_i^T G_i\right)^{-1} G_i^T - \left(G_j^T G_j\right)^{-1} G_j^T\right] \varepsilon = D_{ij} \varepsilon \end{aligned} \qquad (5)$$

$$\begin{aligned} z_{ij} &= D_{ij} \varepsilon = D_{ij} \left(r + b\right) = D_{ij} r + D_{ij} b \\ \overline{z}_{ij} &= D_{ij} E\left(\varepsilon\right) = D_{ij} E\left(r + b\right) = 0 + D_{ij} b = D_{ij} b \end{aligned} \qquad (6)$$

$$\begin{aligned} \sigma_{ij}^2 &= E\left(\left(z_{ij} - \overline{z}_{ij}\right)\left(z_{ij} - \overline{z}_{ij}\right)^T\right) = E\left(\left(D_{ij}\varepsilon - D_{ij} b\right)\left(D_{ij}\varepsilon - D_{ij} b\right)^T\right) = E\left(D_{ij} r r^T D_{ij}^T\right) \\ \sigma_{ij}^2 &= E\left(D_{ij} r r^T D_{ij}^T\right) = E\left(\left[\left(G_i^T G_i\right)^{-1} G_i^T - \left(G_j^T G_j\right)^{-1} G_j^T\right] r r^T \left[\left(G_i^T G_i\right)^{-1} G_i^T - \left(G_j^T G_j\right)^{-1} G_j^T\right]^T\right) \end{aligned} \qquad (7)$$

If the random errors are independent and identically distributed, the variance is given by Equation 8.

$$R = rr^T = I\sigma^2$$
$$\sigma_{ij}^2 = \left(\left[\sigma^2\left(G_i^T G_i\right)^{-1} + \sigma^2\left(G_j^T G_j\right)^{-1} - \sigma^2\left(G_j^T G_j\right)^{-1} G_j^T G_i \left(G_i^T G_i\right)^{-1} - \sigma^2\left(G_i^T G_i\right)^{-1} G_i^T G_j \left(G_j^T G_j\right)^{-1}\right]\right) \quad (8)$$

Similarly, we can determine the solution separation for the faulted (cycle slip) case. For each possible fault (a cycle slip forward and back in time on each station), conduct the analysis as detailed in the fault free case. That is, determine the mean and variance of the solution separation for all possible combinations of nominal bias with the fault. As one can see, this becomes increasingly computationally intensive. If there are ten stations, the one fault case requires that ten cycle slip cases with two possible signs are examined for each possible combination of biases. Because the slip can be forward or back in time, we need to test two possible signs. Thus, for one fault, we need to examine a total of $2*n*2^{n-1}$ different cases, where n is the number of stations or measurements. For two fault combinations, the number of cases that needs to be examined increases to $2*C(n,2)*2^{n-1}$ cases. The factors of two are for the sign (direction) of each of the cycle slip and is C(n,2) is the number of two combinations given n elements.

CYCLE SLIP HYPOTHESIS TESTING

The result from the formulation above is that a worst case solution separation mean and variance is known. The solution separation distribution is Gaussian provided that the measurement error is Gaussian. Standard hypothesis testing can be conducted by looking at the distribution of the faulted (faulted case denoted by subscript 1) compared to that of the nominal (nominal case is denoted by subscript 0). This is seen in Equation (9). k_{UC} corresponds to the complementary cdf (ccdf) probability level for undetected cycle error (P_{UC}) and k_{FAC} corresponds to the Gaussian cdf probability level desired for false alarm of cycle error (P_{FAC}). If the metric, h, is greater than zero for all cases, then the desired level of undetected cycle error and false alarm are met.

$$h = \left(\overline{z}_{ij,1} - k_{UC}\sigma_{ij,1}\right) - \left(\overline{z}_{ij,0} + k_{FAC}\sigma_{ij,0}\right) \geq 0 \quad (9)$$

IMPLEMENTATION

There are a variety of ways the algorithms could be utilized. As both algorithms perform the same function and provide the same output (confidence level on cycle selection), they are represent the same processing blocks in an overall approach to validating Loran cycle selection.

In user equipment, an implementation would proceed as follows. The implementation approach is seen in Figure 1. Start by examining the TOAs or pseudoranges and their corresponding SNR to see if the signals from at least three stations have SNRs above a threshold (i.e. are trusted or form a "trusted triad"), a least squares position is calculated from these trusted signals. This fix is considered a trusted (but not final) fix. If there does not exist three stations with SNRs above a threshold for being trusted, then perform the cycle confidence algorithm. Start by adding a fourth signal (N=4). For SSE, calculate the observability matrix A. If the geometry guarantees detection of cycle errors, or if the cycle errors that cannot be detected are only on trusted signals, the receiver would do preliminary least squares fix and perform a residual test. If, neither of these criteria is satisfied, then repeat with signals from the fifth, sixth, etc. stations, until either one of these two criteria is satisfied, or the receiver determines it cannot obtain a trusted fix. For solution separation, calculate the solution separation and distributions for these four stations and perform the hypothesis test given in Equation 9. One only needs to consider faults on signals that are not "trusted". If the hypothesis test fails, then repeat with signals from the fifth, sixth, etc. stations, until it is passed. Since solution separation becomes increasingly computationally intensive, a pragmatic approach is to limit the maximum number of stations to examine (N_{max}) before N becomes too large. Failure is presumed if the limit is reached without adequate confidence.

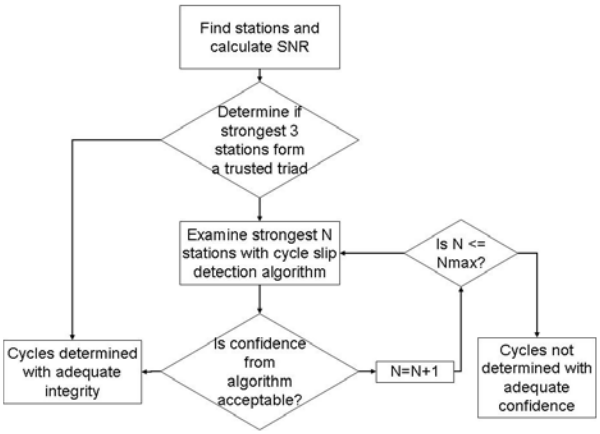

Figure 1. Implementing cycle confidence algorithms

When and if a trusted least squares fix is obtained, the receiver can add any additional signals that could improve accuracy of final fix, first checking to see if the TOA agrees with trusted fix. The final fix is a weighted least square (WLS) fix using all trusted signals.

VALIDATION

There are several means to determine the utility of the algorithms. One method is to use a geometry based study on the major ports through the contiguous United States (CONUS) with Loran coverage. This was conducted on the SSE algorithm.

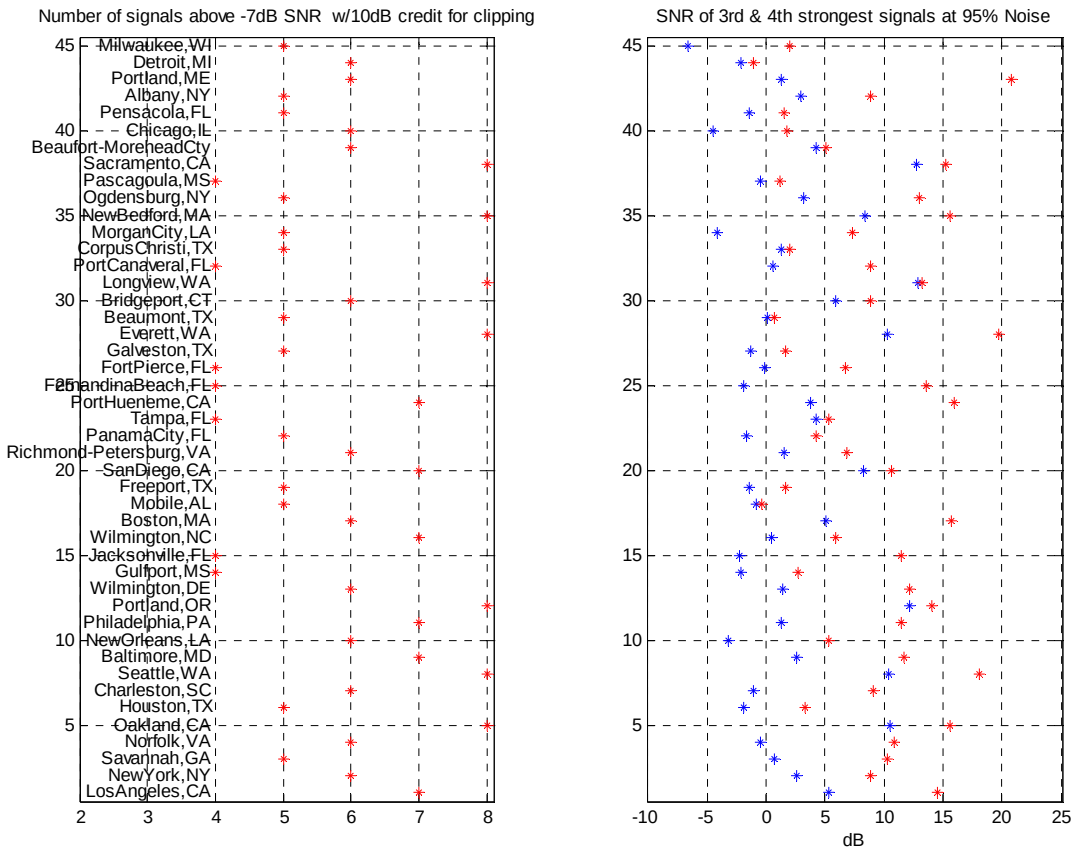

Figure 2. Loran Signal levels at 45 selected ports in CONUS

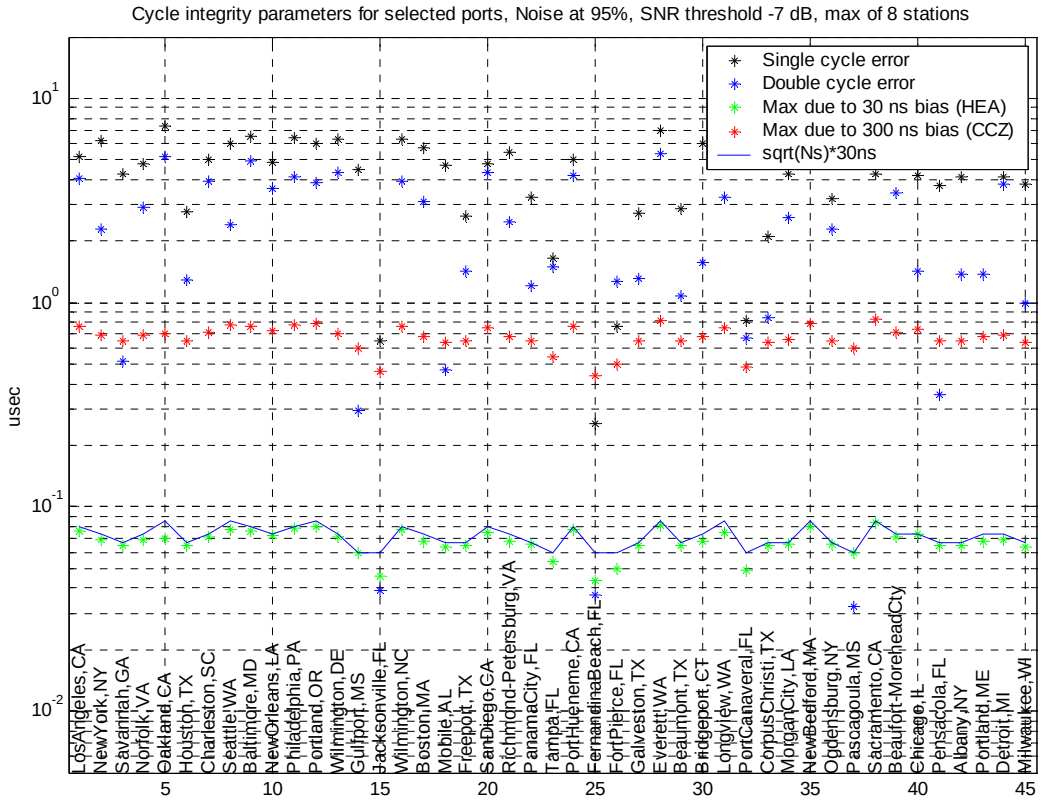

Figure 3. Cycle Integrity Parameters for selected ports

Second, a study of expected availability and performance of the algorithm can also be conducted using Loran Coverage Availability Simulation Tool (LCAST). LCAST was modified to perform solution separation and its hypothesis testing. The tool was then used to examine the availability of the algorithm throughout the CONUS. Both single and double faults with cycle selection are considered. This study helps us determine the coverage limitations of the algorithms.

GEOMETRY STUDY OF PORTS

External to user equipment, a system provider could use the algorithm to analyze whether sufficient signals in space exist to enable HEA *eLoran* operations in a specific port or a regulating agency could use it specify acceptable constellations for that port. To illustrate both how the algorithm works and how HEA availability can be analyzed using the algorithm it will be applied using the expected signals from a number of the largest container ports in conterminous United States (CONUS).

The U.S. Maritime Administration (MARAD) website was used to determine the largest container ports. Starting with the 73 largest container ports, ports in Hawaii, Puerto Rico, and South Florida were eliminated due to the well known lack of *eLoran* coverage in these areas. Duplicates (multiple terminals in same area, etc.) were also eliminated. Also, no Alaska ports were considered.

Analysis of the 45 remaining ports is shown in the following figures. On the left side of Figure 2, these 45 ports are listed starting with the largest port at the bottom. The 95% noise containment level with 10 dB credit for non-linear processing of impulse noise is used for Figure 2. For 99% noise containment the noise is 6.5 dB higher and therefore the SNR's 6.5 dB worse. The red asterisks in right side of Figure 2 show the SNR's of the third strongest signal and indicate whether or not a trusted fix can be obtained with merely a triad. At the 95% noise level, all but approximately three ports have the signals from three or more stations above 2 dB SNR and a trusted fix could be obtained.

Figure 3 applies the algorithm to these 45 ports and shows whether or not a single or double cycle error could be detected if it existed. The black asterisks show the minimum length residual vector for a single cycle error, the blue show this minimum length for any combination two cycle errors of either the same or opposite sign. The green and red asterisks show the maximum length residual vector when the pseudorange errors are bounded by a 30 ns and 300 ns bound respectively.

What we see is that in the case of Detroit, where the third strongest signal has the poorest SNR of any of the 45 ports (Figure 2), there is no problem detecting either a single or double error.

According to Figure 2, the third strongest station at Mobile also has a somewhat poor SNR and a trusted triad fix would not be available, particularly at the 99% noise containment level. In Figure 3, it can be seen that a double cycle may not be detectable at Mobile. Figure 4 shows the azimuths and SNR's of the stations available at Mobile. The first number after the station name is the SNR at the 99% noise level and the second the SNR at the 95% level. At Mobile, the most difficult double error to detect is errors on Grangeville and Jupiter with opposite signs. However, this error not possible due to the SNR of Grangeville.

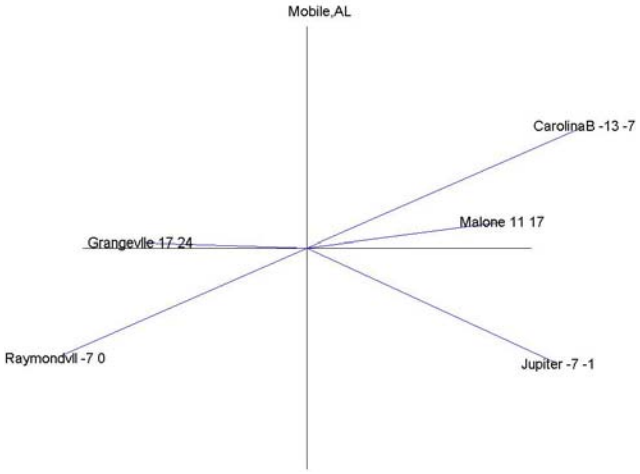

Figure 4. Azimuths and SNR's of Loran stations seen at Mobile.

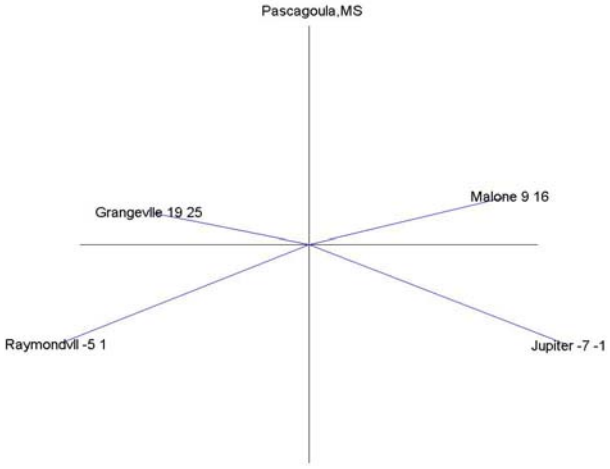

Figure 5. Azimuths and SNR's of Loran stations seen at Pascagoula.

Figure 5 shows the same information at Pascagoula where as with Mobile, figure 1 indicated a low SNR on the third station and figure 2 indicated difficulty in detecting a double error. However, just as with Mobile, the most difficult double error to detect is errors on Grangeville

and Jupiter with opposite signs and this error not possible due to the SNR of Grangeville.

Figure 3 also indicates that both a single error and a double error could not be detected at Fernandina Beach, FL. Figure 6 shows the constellation at Fernandina Beach. The single errors that cannot be detected are on Jupiter and Carolina Beach, and the undetectable double error is errors on Jupiter and Carolina Beach with the same sign. Again, due to SNR's these errors or combination of errors are precluded by high SNR.

In general, it can be seen that both single and double errors can be detected in differential Loran case or undetectable errors precluded by high SNR

In the offshore case, in some locations, it may be possible only to detect a single error, but not double errors.

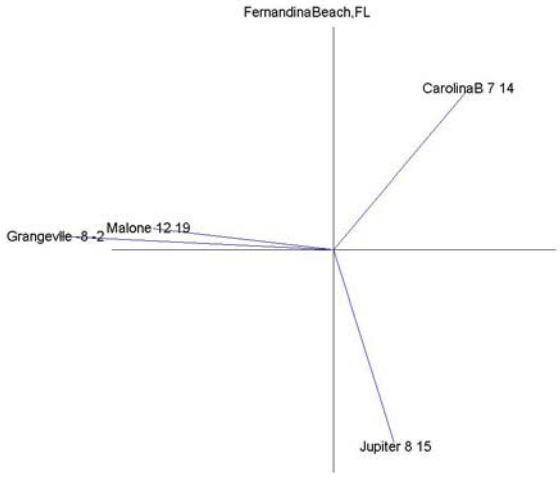

Figure 6. Azimuths and SNR's of Loran stations seen at Fernandina Beach.

COVERAGE SIMULATION STUDY

Solution separation was implemented in LCAST in several ways. First, it was implemented in a manner similar to that given in Figure 1. In this case, solution separation was conducted only if a trusted triad or solution cannot be determined first. There are a few differences from the method described in the prior section. First, given the computational complexity of examining a multitude of stations and faults, the solution separation implementation utilized only the top five strongest stations when available. Essentially, this means N = 4 (if only 4 stations are available) or 5 and N_{max} = 5. Additionally, a trusted station was still tested using solution separation unless there was a trusted triad.

The result of this implementation can be seen in the next 2 figures. Figure 7 shows the implementation given no bias errors, 5% probability of missed detection of a false alarm of cycle error (P_{FAC}) and 0.001% probability of an undetected cycle error (P_{UC}). The simulation assumes a maritime receiver averages for 60 second to determine cycles. Parameters that were examined in the analysis were the effects of bias size and P_{FAC}. Note that a lower P_{FAC} may be acceptable once cycle confidence is determined initially it only needs to be intermittently verified. So, provided noise is not correlated between each attempt, a P_{FAC} of 20% would result in an availability of 99.8% (that is 1 - 0.2^3) over three trials (minutes). Analysis was performed for different biases up to 50 m and P_{FAC} of up to 20%. The end result of the analysis is that there is little variation in coverage despite varying the P_{FAC} and the bias. This can be seen by comparing Figure 7 with Figure 8 which is assumes biases at 50 m instead of 0 m. The reason for this is that the cycles are generally being verified by having a trusted triad which does not depend on these factors.

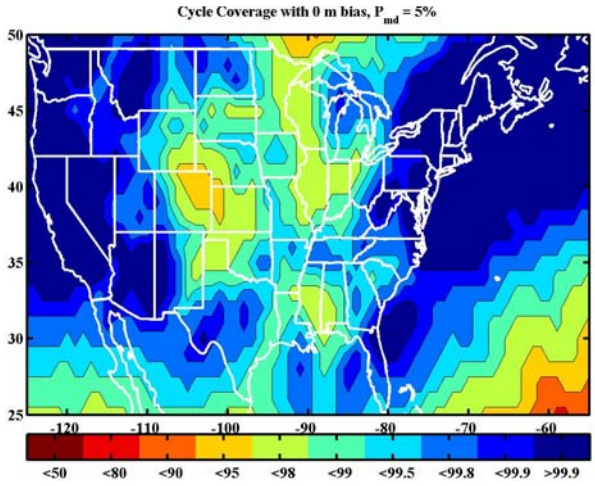

Figure 7. Cycle Coverage Algorithm with P_{FAC} = 5% and 0 m bias

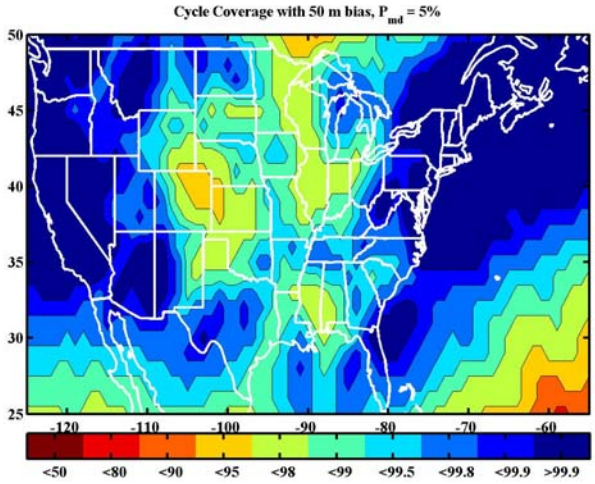

Figure 8. Cycle Coverage Algorithm with P_{FAC} = 5% and 50 m bias

As with the port study, trusted triads provide much of the cycle verification. This is not surprising since the same

underlying noise model and clipping credit is used by LCAST. Given that the prior results came predominately from using trusted triads, the performance of the algorithm without using trusted triads is also tested in LCAST. In this implementation, only the solution separation is utilized. Figure 9 and Figure 10 show the solution separation only results for bias error cases of 0 and 5 m, respectively. Both utilize a P_{FAC} of 5% and a P_{UC} of 0.001%. Solution separation has reasonable availability on the coasts with some noticeable exceptions such as Florida. Additionally, there are "spots" of poor availability likely due to geometry. In Figure 11, the effect of changing the P_{FAC} to 20% and P_{UC} of 0.01% are seen. The resulting coverage is not very different from the previous 2 figures. Analysis suggests that the low availability areas may be due more to geometry than the selected levels for false alarm of cycle error or undetected cycle error.

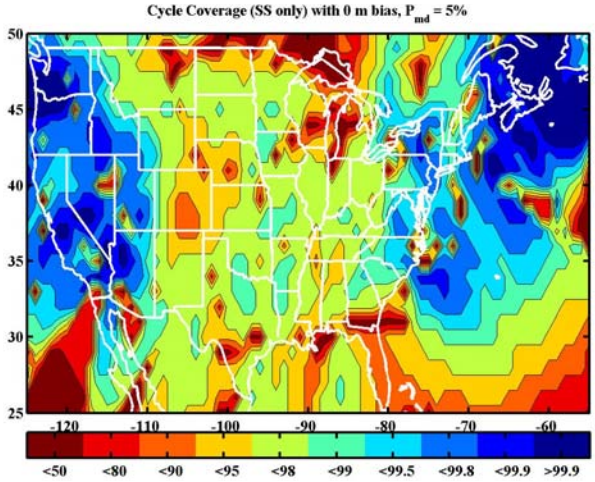

Figure 9. Solution Separation Cycle Coverage Algorithm Only with P_{FAC} = 5% and 0 m bias

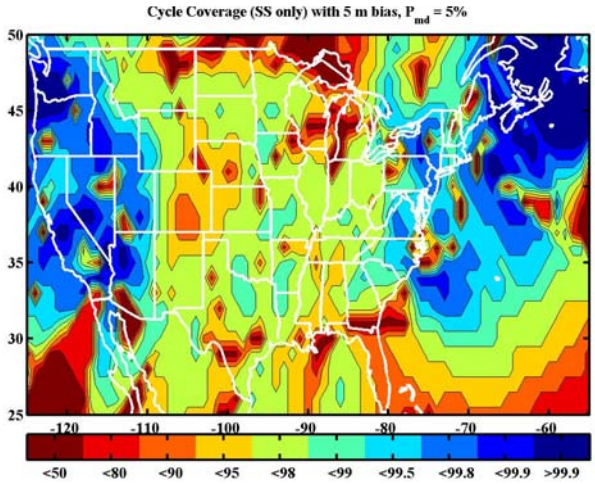

Figure 10. Solution Separation Cycle Coverage Algorithm Only with P_{FAC} = 5% and 5 m bias

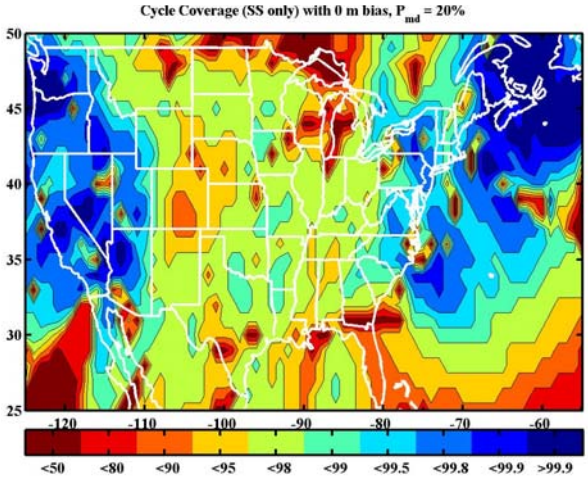

Figure 11. Solution Separation Cycle Coverage Algorithm Only with P_{FAC} = 20%, P_{UC} = 0.01% and 0 m bias

CONCLUSIONS

This paper develops the two algorithms for determining cycle confidence when using differential Loran. The primary benefit of these algorithms is that it is much easier to implement in receiver than the previous WSSE based algorithm. This is critical for keeping computational requirements and hence costs reasonable for receiver manufacturers.

The analysis shows that regardless of whether solution separation or residuals are used, trusted triads will provide the majority of the cycle verification. However, trusted triads are not always available and it is vital to have another algorithm to validate cycles. Both sum square error and solution separation seem to have acceptable availability in coastal ports. The sum square error (residual) method is easier to implement and less computationally intensive. The integrity of the solution separation method can be computed more readily.

ACKNOWLEDGMENTS

The authors would like to thank the FAA Loran Evaluation Program and its Program Manager, Mitch Narins. Additionally, we would like to acknowledge Robert Markle and RTCM Special Committee 127.

DISCLAIMER

The views expressed herein are those of the authors and are not to be construed as official or reflecting the views of the U.S. Coast Guard, Federal Aviation Administration, U. S. Department of Transportation or Department of Homeland Security.

REFERENCES

[1] Lo, Sherman C., Peterson, Benjamin B., Enge, Per K., "Proving the Integrity of the Weighted Sum Squared Error (WSSE) Loran Cycle Confidence Algorithm", Navigation: The Journal of the Institute of Navigation, Vol. 54 No. 4, 2007

[2] Pervan, Boris S., Pullen, Samuel S., and Christie, Jock R., "A Multiple Hypothesis Approach to Satellite Navigation Integrity," Navigation: The Journal of the Institute of Navigation, Vol. 45, No. 1, 1998

[3] Blanch, Juan, Ene, Alex, Walter, Todd and Enge, Per, "An Optimized Multiple Hypothesis RAIM Algorithm for Vertical Guidance," Proceedings of the Institute of Navigation GNSS Conference, Fort Worth, TX September 2007

[4] Peterson, Benjamin, Lo, Sherman and Enge, Per, "Integrating Loran and GNSS for Safety of Life Applications," Proceedings of the Institute of Navigation GNSS Conference, Savannah, GA, September 2008